

Tailoring magnetic vortices in nanostructures

F. Garcia,^{1,a)} H. Westfahl,¹ J. Schoenmaker,¹ E. J. Carvalho,¹ A. D. Santos,² M. Pojar,³ A. C. Seabra,³ R. Belkhou,^{4,5} A. Bendounan,⁴ E. R. P. Novais,⁶ and A. P. Guimarães⁶

¹Laboratório Nacional de Luz Síncrotron, Campinas, 13083-970 São Paulo, Brazil

²LMM, IFUSP, São Paulo, 05508-900 São Paulo, Brazil

³LSI-PSI, Poli-USP, São Paulo, 05508-900 São Paulo, Brazil

⁴Synchrotron SOLEIL, F-91192 Gif-sur-Yvette Cedex, France

⁵Elettra Synchrotron, 34149 Trieste, Italy

⁶CBPF, Rio de Janeiro, 22290-180 Rio de Janeiro, Brazil

(Received 5 March 2010; accepted 18 June 2010; published online 12 July 2010)

Tailoring the properties of magnetic vortices through the preparation of structured multilayers is discussed. The dependence of the vortex core radius r on the effective anisotropy is derived within a simple model, which agrees with our simulations. As the perpendicular anisotropy increases, r also increases until a perpendicular magnetization appears in the disk rim. Co/Pt multilayer disks were studied; x-ray microscopy confirms qualitatively the predicted behavior. This is a favorable system for implementing vortex-based spin-transfer nano-oscillator devices, with enhanced rf power resulting both from the increase in the core size and synchronization afforded by the coupling of the Co layers. © 2010 American Institute of Physics. [doi:10.1063/1.3462305]

In nanomagnetic samples the magnetic domain configuration depends on several parameters of the system such as size, shape, anisotropy, magnetic exchange stiffness, interface roughness, etc. A magnetic vortex often represents the lowest energy configuration,¹ being characterized by the following features: polarity (up or down direction of the vortex core) and circulation (clockwise or counterclockwise curling direction). Vortices have drawn great interest among researchers dealing with nanostructured materials.² Their technological applications are numerous, encompassing from devices such as vortex random access memories^{3,4} to bio-functionalized microdisks for cancer treatment.⁵ They also represent a key system to understand magnetism in reduced dimensions; e.g., a vortex-antivortex square lattice was proposed as a laboratory system for the study as an analog to the Bose–Einstein condensation.⁶

Another application is vortex-based spin transfer nano-oscillators (VSTNOs), used as microwave generator devices and suitable for device integration.^{7–9} Despite their great appeal, these devices generate low power and dissipate much heat. It was demonstrated experimentally,⁶ that the microwave power can be increased through phase-locking of closely spaced nano-oscillators. Still lacking is optimizing the synchronization of these devices. To face these challenges, a fine engineering of the vortex features and optimizing device geometry is highly desirable. Many efforts have been made in order to modify the vortex properties,¹⁰ however, properties such as vortex core size are hard to adjust and highly dependent on the magnetic anisotropies of the system.¹¹

In Co/Pt multilayer systems the effective magnetic anisotropy (K_{eff}) is sensitive to the interface contributions, and can be easily controlled from in-plane to out-of-plane by playing with the Co thickness [e.g., see Ref. 12]. Moreover, these systems have been shown to present TMR or GMR.^{9,13–15} In this letter, we propose Co/Pt multilayer engi-

neering to tailor the Co vortex properties by means of the interface contribution to K_{eff} ; we show how the vortex core magnetization and radius (r) can be tailored by controlling K_{eff} .

According to studies on single-layered structures, typically vortices cores have $r \sim 5$ nm. In the limit of small thickness ($t \rightarrow 0$), r can be expressed by¹⁶ $\sqrt{A/K_d}$, where A is the exchange stiffness and K_d is the magnetostatic energy density ($K_d = \mu_0 M_s^2/2$). The effective anisotropy K_{eff} in Co/Pt multilayers can be described by the following phenomenological expression:

$$K_{\text{eff}} = K_v - 2(K_s/t), \quad (1)$$

where t is the Co thickness, K_v and K_s are the volume and interface anisotropy, respectively. From Eq. (1), one sees that it is possible to vary K_{eff} of a multilayer, simply by varying t ; as K_{eff} crosses zero, there is a spin reorientation, from in-plane ($K_{\text{eff}} > 0$) to out-of-plane ($K_{\text{eff}} < 0$).¹²

Following Ref. 16, we used the ansatz for the core magnetization of a vortex, in cylindrical coordinates; $m_z = m_z(\rho) = \exp(-2\beta^2\rho^2)$, where β is the variation parameter, corresponding to $1/2r$. We have considered no in-plane anisotropy, only perpendicular anisotropy energy, proportional to the perpendicular anisotropy constant K_z as follows:

$$E_z = -2\pi K_z t \int \rho d\rho m_z^2 = \pi K_z t \frac{[\exp(-4D^2\beta^2) - 1]}{4\beta^2}. \quad (2)$$

Minimizing the total energy, i.e., exchange, magnetostatic [Eqs. (5) and (8) of Refs. 16, respectively] and perpendicular anisotropy energy, we arrive at the following:

$$\frac{1}{\beta} = 2r = 2\sqrt{\frac{A}{K_d - K_z}}, \quad (3)$$

valid up to the limit r much smaller than the disk diameter D , i.e., $\beta D \gg 1$. Note that in this approximation r diverges for a sufficiently large anisotropy, and for $K_d < K_z$, there is no real solution.

^{a)}Electronic mail: fgarcia@lnls.br.

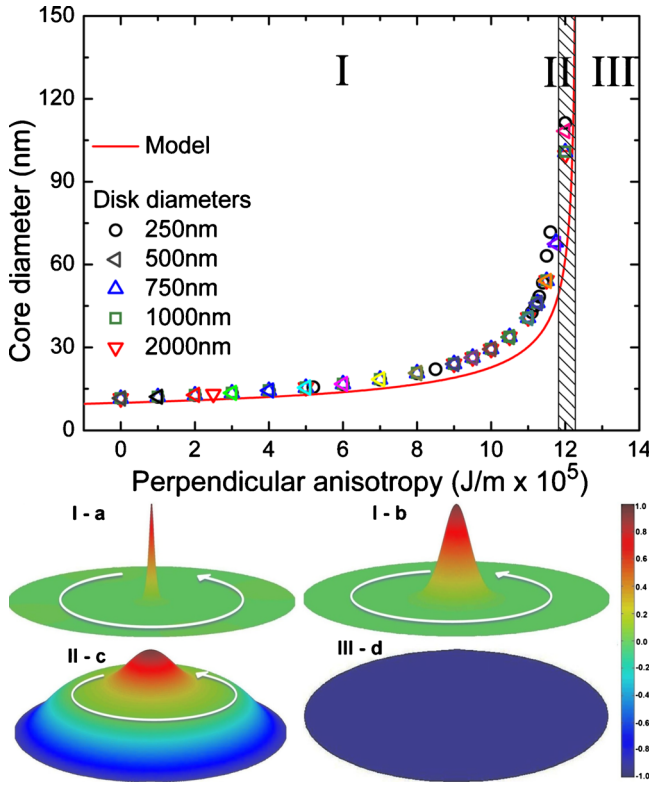


FIG. 1. (Color online) Simulated phase diagram of spin configuration of the Co/Pt multilayer disks as a function of perpendicular anisotropy and disk diameter. [a(i)] narrow core diameter ($K_z=0$). [b(i)] wide core diameter ($K_z=1.18 \times 10^5$ J/m³). [c(II)] annular spin structure ($K_z=1.2 \times 10^5$ J/m³). [d(III)] perpendicular single domain ($K_z > 1.2 \times 10^5$ J/m³).

Considering that K_d and K_z are, respectively, equivalent to the volume anisotropy K_v and the interface term $2K_s/t$ in Eq. (1), in our model r is a function of K_{eff} . Micromagnetic simulations (OOMMF code¹⁷) were performed to verify the model validity. We obtained the ground state configuration for 0.25, 0.5, 0.75, 1, and 2 μm diameter disks of a single Co layer as a function of the perpendicular anisotropy constant (K_z). The cell size was taken as $2 \times 2 \times 2$ nm³; $A=30 \times 10^{-12}$ J/m and $M_s=1400 \times 10^3$ A/m (the values used for bulk Co). Again, we have considered only the perpendicular term in the simulations; r was determined from a pseudo-Voigt function fit to $m_z(\rho)$ obtained from the simulation.

Our simulations (Fig. 1) show vortices when K_z is included, pointing to the possibility of obtaining vortices in Co/Pt multilayer disks. A more relevant conclusion is that r varies as a function of K_z , following the behavior predicted by our model [Eq. (3)]. A phase diagram (Fig. 1) displays core size versus K_z (and therefore Co thickness) for $D=250$, 500, 750, 1000, and 2000 nm [Eq. (3) is also plotted]. A good agreement between the core diameters is obtained for the simulation and our model [Eq. (3)] for all disk diameters investigated. From this phase diagram, we can distinguish three regimes. For low values of K_z (region I, Fig. 1), we find an ordinary vortex structure with nearly the expected vortex core diameter (~ 10 nm) for a soft magnetic micrometric disk, i.e., for $K_z=0$ [I-a in Fig. 1]. In region I, we observe a monotonic increase in the diameter as a function of K_z , as predicted by the model. The increase in $2r$ is extended up to the limit of validity given by Eq. (3) [I-b of Fig. 1], followed by region II in the graph of Fig. 1. In region II, we observe that by augmenting the interface contribution, the spin con-

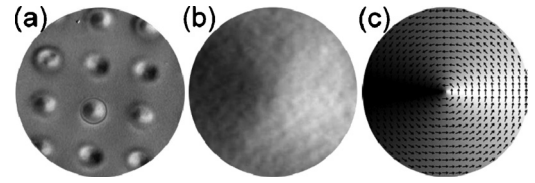


FIG. 2. (a) Image obtained by XMCD-PEEM of the $[\text{Co}_2/\text{Pt}_2] \times 6$ 1 μm disk array. (b) Detail of the disk highlighted by the red circle, presenting a typical vortex pattern. (c) OOMMF simulation of a disk with the same characteristic, showing a good agreement with (a).

figuration may present increasingly out-of-plane components. Besides the perpendicular magnetization of the vortex core, a perpendicular magnetization also appears at the rim of the disks [II-c in Fig. 1], forming a domain configuration of out-of-plane concentric rings. Although K_v is still larger than $2K_s/t$, the boundary conditions impose an out-of-plane K_{eff} . Region III: for $2K_s/t > K_v$, it gives rise to an out-of-plane single domain [region III and III-d of Fig. 1], and therefore the vortex is no longer observed.

Four samples, consisting of lithographed arrays of Co/Pt multilayered disks [$D=1$ and 2 μm] deposited by sputtering on $\text{SiO}_2/\text{Si}(100)$ wafers, were produced. Their structure was $([\text{Co}_t/\text{Pt}_2]_6/\text{Pt}_6)$ with Co layer thickness $t=2.0$, 1.6, 0.8, and 0.6 nm. Continuous films were also produced in the same sputtering runs. The magnetic properties and morphology of the samples were characterized by magnetometry, x-ray magnetic circular dichroism (XMCD) photoelectron emission microscopy (PEEM) and magnetic force microscopy.

The XMCD-PEEM measurements were performed at the Nanospectroscopy beamline at Elettra Synchrotron, Italy. The final pictures were obtained by averaging up to 250 images (taken at Co L_3 edge) originated from subtracting two images acquired with opposite (left/right) circular polarizations. This imaging technique contrasts the magnetization alignment relative to the x-ray beam direction. The experiment was carried out in grazing incidence setup (16°), therefore the images distinguish mostly the in-plane magnetization distribution, the black/white contrast referring to parallel/antiparallel relation between the magnetization components and the beam direction. However, the measurements are still sensitive to the perpendicular magnetization, due to the angle between the perpendicular magnetization and the x-ray beam.

Figure 2 shows images of the $[\text{Co}_2/\text{Pt}_2] \times 6$ multilayered disks, which presented the highest K_{eff} . For the 1 and 2 μm array, almost all disks have a single vortex structure. This is confirmed if we compare the experimental result of a particular disk size with the equivalent simulated one (Fig. 2). The realization of magnetic vortices in a multilayer system represents a great step toward better controlling the magnetic vortex properties and characteristics.

For the arrays with a smaller Co thickness $[\text{Co}_t/\text{Pt}_2] \times 6$ ($t=0.6$ and 0.8 nm), i.e., for $K_{\text{eff}} \sim 0$, the magnetic configurations do not seem to correspond to an usual vortex [XMCD-PEEM image in Fig. 3(a)]. In this case, it is observed a smaller bright/dark contrast close to the center. Our interpretation is that we have the same spin configuration of region II of the phase diagram [see II-c in Fig. 1], i.e., at the center M is pointing upwards, at the rim downwards and in-between there is a planar vortex. For comparison, Fig. 3(b) also presents the spin configuration of c(II) (Fig. 1), but

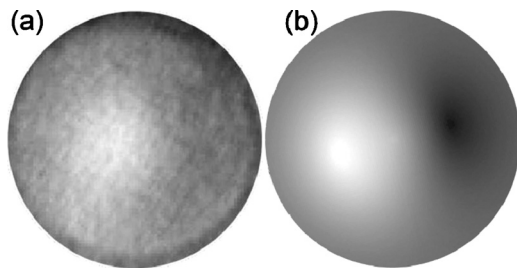


FIG. 3. (a) XMCD-PEEM image of $1\ \mu\text{m}$ $[\text{Co}_{0.6}/\text{Pt}_2] \times 6$ disk. (b) simulated spin configuration of a disk of the same size (region II in the phase diagram of Fig. 1), showing a good agreement with (a).

in a pattern that mimics the PEEM contrast, showing a good agreement between the measurement and the simulation. In this case, the faint contrast is due to the 16° tilt angle between the plane of the sample and the x-rays direction.

Although the XMCD-PEEM technique is not well suited for assessing r , we could observe a behavior that corroborates our proposition. For the thicker Co layers, where it is expected a larger in-plane anisotropy, we obtained a vortex structure (Fig. 2). As we get closer to the spin reorientation transition condition, i.e., for thinner Co layers, we observed out-of-plane magnetization in concentric annular regions (Fig. 3). This agrees with the simulations, i.e., vortex structure and annular arrangement, corresponding to regions I and II (Fig. 1).

These results open up opportunities for optimizing VSTNOs devices.⁶ The magnetic dipole moment of the vortex core is proportional to its square radius (r); $\mu = \pi r^2 t M_s$. The synchronization of the gyrotropic motion of the cores in an array of vortices⁶ is dependent on the coupling between vortices through the antivortices, and therefore dependent on the dipolar and long-range exchange interactions between vortices and antivortices counter balanced by the restoring forces (Oersted field). Since both interactions depend on r , tailoring r is relevant for increasing the microwave power and for achieving phase locking in VSTNOs.

Maybe the most significant contribution of multilayer-based vortex systems would be the establishment of an alternative architecture for the VSTNOs, i.e., a vertical vortices stacking, possibly solving the problems of synchronization and power. This vortices stacking device is naturally phase-locked, since it is well-known that the Co layers are coupled,¹⁸ and therefore the power generated will be amplified relative to an individual vortex. Hence, we would have a

synchronized set of vortices in a very compact device.

In conclusion, tailoring magnetic vortex core diameters as well as other properties of magnetic disks is proposed by adjusting the interface energy contribution in Co/Pt multilayered structured system. The proposal is supported by a model and by micromagnetic simulations which present consistent results. Theory and simulation are also presented in the form of a phase diagram defining three regions with distinct domain structure. We demonstrated experimentally vortex formation on Co/Pt multilayered disks. We also verified that vortex nucleation is affected by the interface contribution, consistently with the model. Finally, we proposed and demonstrated a strategy to engineer magnetic vortex properties to suit technological application demands.

We thank FAPESP, CNPq, FAPERJ, LNLS, and Elettra for financial support.

- ¹A. P. Guimarães, *Principles of Nanomagnetism* (Springer, Berlin, 2009).
- ²C. L. Chien, F. Q. Zhu, and J.-G. Zhu, *Phys. Today* **60**(6), 40 (2007).
- ³S.-K. Kim, K.-S. Lee, Y.-S. Yu, and Y.-S. Choi, *Appl. Phys. Lett.* **92**, 022509 (2008).
- ⁴S. Bohlens, B. Krüger, A. Drews, M. Bolte, G. Meier, and D. Pfannkuche, *Appl. Phys. Lett.* **93**, 142508 (2008).
- ⁵D.-H. Kim, E. A. Rozhkova, I. V. Ulasov, S. D. Bader, T. Rajh, M. S. Lesniak, and V. Novosad, *Nature Mater.* **9**, 165 (2010).
- ⁶A. Ruotolo, V. Cros, B. Georges, A. Dussaux, J. Grollier, C. Deranlot, R. Guillemet, K. Bouzehouane, S. Fusil, and A. Fert, *Nat. Nanotechnol.* **4**, 528 (2009).
- ⁷D. V. Berkov and N. L. Gorn, *Phys. Rev. B* **80**, 064409 (2009).
- ⁸R. Lehnndorff, D. E. Bürgler, S. Gliga, R. Hertel, P. Grünberg, C. M. Schneider, and Z. Celinski, *Phys. Rev. B* **80**, 054412 (2009).
- ⁹D. Houssameddine, U. Ebels, B. Delaet, B. Rodmacq, I. Firastrau, F. Ponthenier, M. Brunet, C. Thirion, J.-P. Michel, L. Prejbeanu-Buda, M.-C. Cyrille, O. Redon, and B. Dieny, *Nature Mater.* **6**, 447 (2007).
- ¹⁰M. M. Soares, E. De Biasi, L. N. Coelho, M. C. dos Santos, F. S. de Menezes, M. Knobel, L. C. Sampaio, and F. Garcia, *Phys. Rev. B* **77**, 224405 (2008).
- ¹¹T. S. Machado, T. G. Rapoport, and L. C. Sampaio, *Appl. Phys. Lett.* **93**, 112507 (2008).
- ¹²M. T. Johnson, P. J. H. Bloemen, F. J. A. den Broeder, and J. J. de Vries, *Rep. Prog. Phys.* **59**, 1409 (1996).
- ¹³F. Garcia, F. Fetta, S. Auffret, B. Rodmacq, and B. Dieny, *J. Appl. Phys.* **93**, 8397 (2003).
- ¹⁴B. G. Park, J. Wunderlich, D. A. Williams, S. J. Joo, K. Y. Jung, K. H. Shin, K. Olejnik, A. B. Shick, and T. Jungwirth, *Phys. Rev. Lett.* **100**, 087204 (2008).
- ¹⁵J.-H. Park, M. T. Moneck, C. Park, and J.-G. Zhu, *J. Appl. Phys.* **105**, 07D129 (2009).
- ¹⁶P.-O. Jubert and R. Allenspach, *Phys. Rev. B* **70**, 144402 (2004).
- ¹⁷M. J. Donahue and D. G. Porter, <http://math.nist.gov/oommf/>.
- ¹⁸J. Moritz, F. Garcia, J. C. Toussaint, B. Dieny, and J. P. Nozières, *Europhys. Lett.* **65**, 123 (2004).